Carbon Nitride as a Buffer Layer for Magnetic Thin Films

S. Watson[1], L. Zeng[2], J. Musielski[1], R. Wincheski[3], A. Wilkerson[2], E Broitman[2],

B. Holloway[2] and A. Reilly[1]

1.Department of Physics, The College of William and Mary, Williamsburg, Virginia 23187
2. Department of Applied Science, The College of William and Mary, Williamsburg, Virginia 23187
3. NASA Langley Research Center, Hampton, VA 23681

Abstract

Amorphous carbon nitride ($CN_{x,\ 0.1<x<0.3}$) thin films present a unique combination of hardness and compliance and may be useful for incorporation into ferromagnetic multilayers. We present a study of the use of amorphous CN_x as a buffer layer for NiFe magnetic thin films. The surface roughness of the NiFe films is comparable to films on Ta or Cu buffer layers and is stable with annealing at 200^{o}C. Effects on the magnetization and coercivity are seen, and may be due to several mechanisms, including chemical reactions at the interface and interdiffusion.

I. Introduction

Amorphous carbon nitride ($CN_{x,\ 0.1<x<0.3}$) has generated interest because of its unique combination of hardness and compliance. Its physical properties: high hardness, low friction coefficient, good chemical inertness, thermal stability and low wear rates make it a suitable choice for many applications.[1,2] Variations in atomic hybridization allow for a spectrum of physical properties based on growth conditions, from a "soft" amorphous-carbon-like material to a "hard" diamond-like structure.[3] CN_x strongly bonds to ordinary Si <100> wafers forming a hard coating,[3] which, along with its band gap structure, might make CN_x useful in electronic and computer applications.[3] CN_x is currently used as a protective coating for hard drive media.[4] CN_x may also be useful when incorporated directly into ferromagnetic multilayer structures (such as those displaying giant or tunneling magnetoresistance) as a buffer, capping or active electronic layer. Its properties may enhance the robustness of the ferromagnetic structure and prevent deterioration due to chemical corrosion or thermal annealing. Also, its excellent thermal properties and varying impedance (based on growth conditions) make it useful for microelectronic devices. For example, a hard carbon layer such as CN_x could be an alternative for the insulating layers in spin-tunneling devices, to replace the standard metal oxides such as Al_2O_3.

Before hard carbon thin films see incorporation into magnetic multilayers, there must be studies of their structural and magnetic effects. Although there have been reports of the effects on magnetization when incorporating diamond-like or amorphous carbon[5] with magnetic thin films or granular films[6,7,8] of CN_x with ferromagnetic elements, there have been no published reports of using CN_x as a buffer layer for magnetic thin films. Studying the interaction between

carbon and magnetic thin films is also of interest given recent reports of carbon magnetism and magnetic proximity effects[9].

II. Experimental Procedures

Deposition of CN_x films was carried out in a high-vacuum dc magnetron sputtering system with a base pressure of ~ 2 X 10^{-7} Torr. Pure nitrogen (99.998%) was introduced in the chamber through a mass flow controller which, combined with turbo pump throttling, maintained a constant chamber pressure of 8 mTorr during deposition. Carbon was sputtered from a high-purity (99.99%) graphite target, 2" in diameter, positioned 10 cm from the substrate holder. The typical discharge current and voltage were 0.3 A and ~ 615 V, respectively. The films were deposited on grounded 4" dia. single-crystal <100> Si substrates. The wafers were initially cleaned in an ultrasonic bath of acetone followed by isopropanol. The substrate temperature was 300^0C during all CN_x depositions. The deposition rate was 9-10 nm/min, as measured by surface profilometry. The thicknesses ranged from 180 to 220 nm across the wafer. Prior to the NiFe deposition , ½ cm by 1cm square cuts were made from the center of the CN_x coated wafer.

High-resolution transmission electron microscopy (HRTEM) has shown that the films were amorphous. Nanoindentation experiments carried out with a Triboscope (Hysitron Inc.), using a cube corner diamond tip with an indentation load of 40 μN, have shown a hardness of ~ 8 GPa and an elastic recovery of 60 %.

In a separate sputtering chamber, NiFe was deposited at room temperature onto the CN_x by dc magnetron sputtering. The CN_x films were placed in the sputtering chamber two days after their growth and were not pre-treated in any way. The chamber base pressure (roughing and cryo-pumped) was 5 x 10^{-8} Torr. The sputtering pressure of argon was 2 mTorr. NiFe layers

with thicknesses of 1, 2, 3, 5, and 10 nm were sputtered from a target of 81% Ni and 19% Fe at a deposition rate of 1 Å/s. As reference samples, NiFe films with 10 nm Cu and Ta buffer layers (at 1 Å/s) were also deposited under the same vacuum conditions. Capping layers were not deposited on any of the samples. After depositing each Si/buffer/NiFe film, the ten films, two for each thickness, were divided into two groups. One group was annealed for four hours in an argon environment at approximately 200°C in a controlled ambient oven with Argon as the process gas. For consistency, each set of Si/x/NiFe films was annealed the day after deposition. Unannealed films were kept in vacuum desiccators to hinder oxidation and water absorption.

SQUID magnetometry (Quantum Design MSPS) was used to measure the magnetization of the NiFe on CN_x, Cu, and Ta buffer layers. Film structure was characterized by atomic force microscopy (AFM-Digital Instruments Nanoscope), scanning and transmission electron microscopy (SEM and TEM) and X-ray diffraction.

III. Results and Discussion

Figure 1 shows AFM scans of a 3 nm NiFe film on a CN_x buffer layer, before and after annealing. The surface for both films is observed to be smooth. Whereas it was difficult to resolve the grains of the NiFe films on the Ta or Cu, the larger grain pattern of the NiFe on the CN_x is obvious. A similar structure was seen in both high-resolution SEM and TEM images. It was found that, before annealing, the 3 nm NiFe films deposited on the CN_x are comparably as rough (Rrms = 2.8 ± 0.6 nm, Ravg = 2.3 ± 0.5 nm, Z = 24.8± 4.5 nm) as those on the Ta (Rrms = 2.4 ± 0.6 nm, Ravg = 1.9 ± 0.6 nm, Z = 21.7 ± 6.8 nm) and Cu buffer layers (Rrms = 2.9 ± 1.8 nm, Ravg = 2.4 ± 1.5 nm, Z = 20.9 ± 15.3 nm). After annealing, the roughness of the CN_x/NiFe actually decreases (Rrms = 1.8 ± 0.1 nm, Ravg = 1.4 ± 0.1 nm, Z = 14.2 ± 1.7 nm), unlike the

films with Cu and Ta buffer layers, where the roughness increases (Rrms = 4.6 ± 2.8 nm, Ravg = 3.8 ± 2.4 nm, Z = 28.9 ± 17.9 nm and Rrms = 5.9 ± 4.2 nm, Ravg = 4.4 ± 3.5 nm, Z = 104.7 ± 30.8 nm respectively). These results are summarized in Table 1. As seen in Figure 1, the grain structure of the CN_x/NiFe does not appear to be significantly altered upon annealing.

Figure 2 shows the magnetization of a 10 nm NiFe film on both a Ta and CN_x buffer layer. The coercivity for the Ta buffer layer is ~ 4 Oe and is thickness independent within ± 1 Oe. As seen in Figure 2, annealing at 200^0C for 4 hours has little change on the hysteresis loop of the NiFe on the Ta buffer layers (similar results were seen with Cu). In contrast, the NiFe film on the CN_x initially has a larger, thickness-dependent coercivity (H_c = 36 Oe for 10 nm of NiFe). Upon annealing, both the saturation magnetization and the coercivity of the NiFe film decrease dramatically (H_c = 11 Oe for 10 nm of NiFe).

Figure 3 shows the saturation magnetization of the NiFe films on the various buffer layers as a function of NiFe film thickness. From this data the thickness of the magnetic dead layer can be estimated. For the unannealed NiFe films on Ta and Cu a dead layer of ~ 1 nm is estimated, which is slightly larger but comparable to that seen with other Ta/NiFe systems[10]. Films with a NiFe thickness of 1 nm on Ta or Cu showed no evidence of hysteresis loops, but only a diamagnetic response. Upon annealing at 200°C for 4 hours, the dead layer does not increase for these buffer layers, indicating that significant interfacial mixing is not occurring. For the CN_x buffer layer, the unannealed films showed a larger dead layer of at least 2 nm. Upon annealing, it is clear that the total magnetization is decreasing, but we do not have enough data points to determine if this is due to an increase in the dead layer. For the NiFe films on CN_x, the unannealed and annealed films with thickness 2 nm and less showed a diamagnetic response.

The saturation magnetization of the NiFe, calculated from linear fits in Figure 3, is highest on the unannealed Ta buffer layer (M_s = 796 emu/cm^3) and decreases with annealing (M_s = 628 emu/cm^3). The magnetization of the NiFe films on the CN_x can be estimated from a linear fit (not shown) if a 2 nm dead layer is assumed. From this, we find M_s=593 emu/cm^3 for the unannealed CN_x/NiFe films and M_s =371 emu/cm^3 for the annealed films. Some of the decrease in magnetization can be attributed to oxidation of the surface of the NiFe, since the films were uncapped. However, it is obvious that the CN_x buffer layer is causing a further decrease in the NiFe magnetization that worsens upon annealing.

Preliminary x-ray diffraction measurements show a strong fcc <111> ordering for the 10 nm NiFe films on the Ta buffer layers. The 10 nm NiFe film on the amorphous CN_x however, showed no strong ordering peaks. TEM measurements indicate a multi-crystalline structure for this film.

The decrease in magnetization and change in coercivity for the CN_x buffer layer are undesirable results for producing a stable magnetic multilayer structure. One possible cause is that the CN_x structure is not stable upon annealing, however, studies have shown that CN_x is stable at this annealing temperature since it is below the growth temperature.[11] Results from AFM, SEM and TEM do not suggest that a structure change is occurring. Upon annealing, the NiFe could be interdiffusing into the CN_x layer, forming a granular structure. In this case, an increase in coercivity may be expected. Another possibility is a combination of intermixing or the formation of nitrides or carbides at the interface. Studies of Ni/C and Fe/C multilayers (where C is amorphous carbon) have shown the formation of Ni_3C and Fe_3C at the interface (Ni_3C decomposes upon heating while Fe_3C is formed with heating).[5] A more significant effect may be that the amorphous CN_x films are hydrophilic and that water is released upon annealing at 150^{o}C,

as shown in recent NMR studies[12]. Given this, oxidation could be occurring in the NiFe film from the released water, which reduces the magnetization. Preliminary data on CN_x/NiFe films has shown that the magnetic properties improve and become more stable when the CN_x is grown at higher temperatures. This could be due to the higher temperature films having less nitrogen content and being less hydrophilic, or the interface bonding may be more stable.

In summary, we have presented a study of the use of amorphous CN_x as a buffer layer for NiFe magnetic thin films. The surface roughness of the films looks comparable to films on Ta or Cu buffer layers and is stable with annealing up to 200^{o}C. A decrease in magnetization and increase in coercivity are seen, as compared to films on Ta and Cu buffer layers, and may be due to several mechanisms, including chemical reactions at the interface or interdiffusion. This present study took place on amorphous CN_x films. Further studies will explore use of fullerene-like CN_x and decreasing the hydrophilic effects of the CN_x.

ACKNOWLEDGEMENTS

We thank Jung Gi Kim of Hanyang University, Korea for preliminary x-ray diffraction results. This work supported by the American Chemical Society Petroleum Research Fund, Research Corporation and AFOSR.

References

1. Li Hong Zhang, Hao Gong, and Jian Ping Wang, J. Physics: Condens. Matter, **14** 1697 (2002).
2. R. Prioli, S.I. Zanette, A.O. Caride, M. M. Lacerda, and F.L. Freire Jr., Diamond and Related Mat., **8** 993 (1999).
3. A. Bousetta, M. Lu, and A. Bensaoula, J. Vac. Sci. Tech. A, **13** 1639 (1995).
4. A. Khurshudov, K. Kato, S. Daisuke, J. Vac. Sci. Tech., **14** 2935 (1996).
5. R. Krishnan, H.O. Gupta, C. Sella and M. Kaabouchi, J. Mag. Magn. Mat., **93** 174 (1991)
6. J.N. Zhou, J. Du, A.F. Khapikov, S. Wang, J.A. Barnard, J.W. Harrell, W.D. Doyle, J. Appl. Phys., **87** 5624 (2000).
7. C. Ruby, J.N. Zhon, J. Du, S.C. Street, J. Barnard, Surface & Interface Analysis, **29** 38-45 (2000).
8. J. Du, S. Wang, J.N. Zhou, J.W. Harrell, J.A. Barnard, Journal of Magnetism & Magnetic Materials, **219** 78-8 (2000).
9. J.M.D. Coey, M. Venkatesan, C.B. Fitzgerald, A.P. Douvalls, I.S. Sanders, Nature, **420**, 156-9 (2002).
10. Qunwen Leng, Hua Han, Ming Mao, Craig Hiner, and Francis Ryan, J. Appl. Phys., **87** 6621 (2000).
11. N. Hellgren, Lin Nian, E. Broitman, V. Serin, S.E. Grillo, R. Twesten, I. Petrov, C. Colliex, L. Hultman, J-E. Sundgren, Journal of Materials Research, **16**, 3188-201(2001)
12. W.J. Gammon, G.L. Hoatson, B.C. Holloway, R.L. Vold, A.C. Reilly, Physical Review B, **68** 195401 (2003).

TABLE and FIGURE CAPTIONS

Table 1. Roughness data (average and rms roughness and peak height, Z) taken by AFM for 3 nm NiFe films on three buffer layers. Measurements were taken on unannealed and annealed films. Note that the roughness of the CN_x/NiFe film significantly decreases upon annealing.

Figure 1. AFM scans for 3 nm of NiFe on CN_x. Left: unannealed sample. Right: annealed sample. Dimension of scan shown is 2.5 micron x 2.5 micron.

Figure 2. Magnetization of 10 nm of NiFe on Ta (left) and CN_x (right) buffer layers. Closed dots are annealed samples, open dots are unannealed samples. Data taken at 200K.

Figure 3. Magnetization versus NiFe layer thickness for various buffer layers, before and after annealing. Lines are linear fits to extract bulk magnetization and dead layer thickness.

	unannealed			annealed		
Film	R_{rms} (nm)	R_{avg} (nm)	Z (nm)	R_{rms} (nm)	R_{avg} (nm)	Z (nm)
Ta/NiFe	2.4 ± 0.6	1.9 ± 0.6	21.7 ± 6.8	5.9 ± 4.2	4.4 ± 3.5	104.7 ± 30.8
Cu/NiFe	2.9 ± 1.8	2.4 ± 1.5	20.9 ± 15.3	4.6 ± 2.8	3.8 ± 2.4	28.9 ± 17.9
CN_x/NiFe	2.8 ± 0.6	2.3 ± 0.5	24.8± 4.5	1.8 ± 0.1	1.4 ± 0.1	14.2 ± 1.7

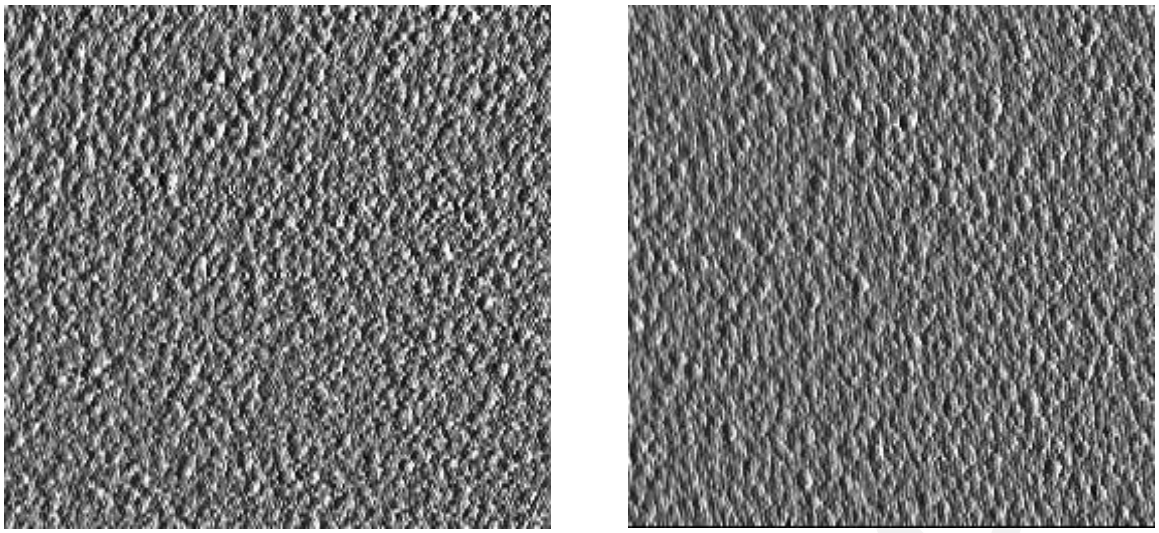

Figure 1.

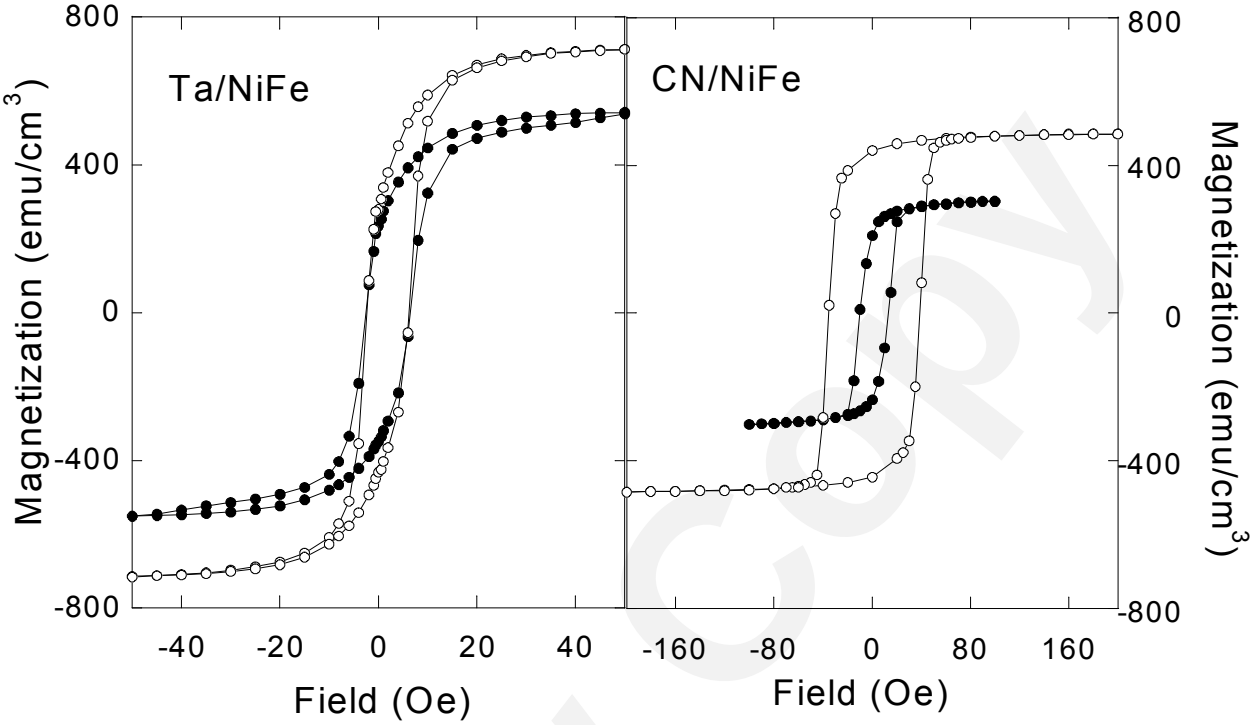

Figure 2.

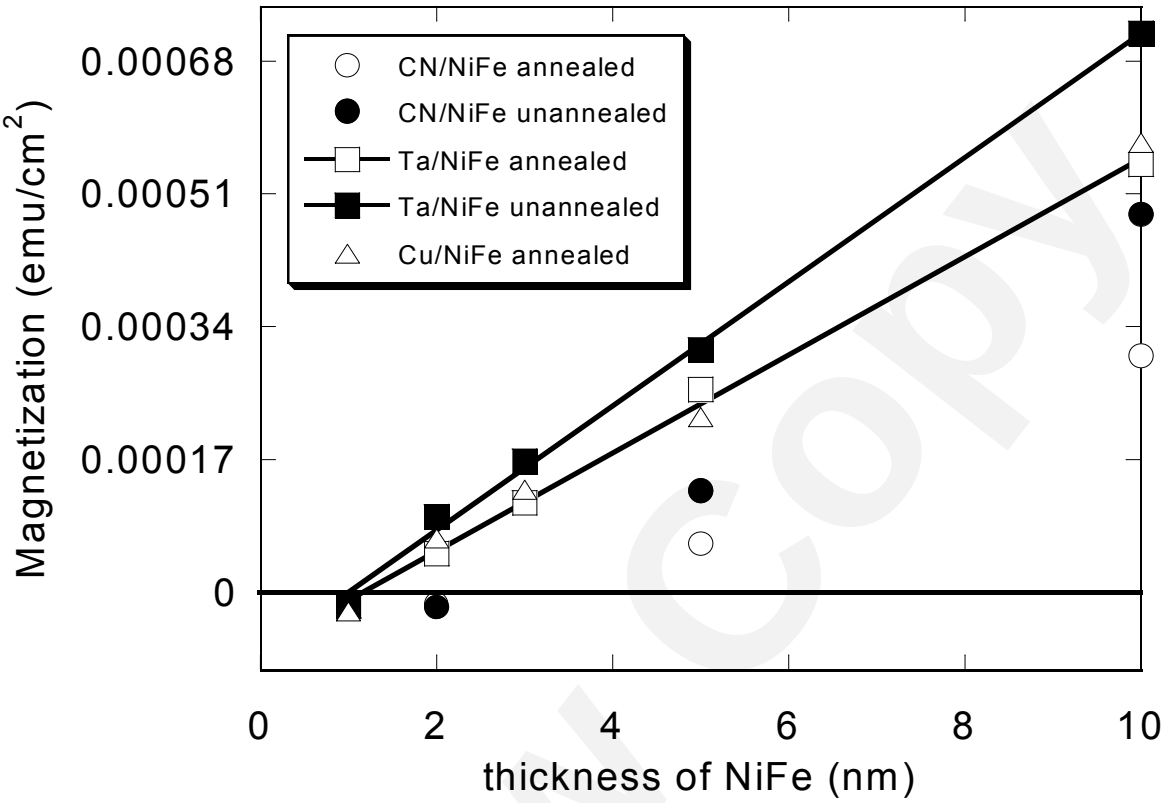

Figure 3.